



# Surface Electrons on Solid Quantum Substrates: A Brief Review

Paul Leiderer<sup>1</sup>

Received: 13 October 2024 / Accepted: 28 February 2025 / Published online: 3 April 2025  
© The Author(s) 2025

## Abstract

In this work an overview is given on experiments with surface electrons above the quantum solids hydrogen and neon. While two-dimensional ensembles of surface electrons on the quantum liquid superfluid helium have been studied already in great detail, investigations of electrons on quantum solids are rather sparse. Since recently electron-on-neon qubits have been shown to exhibit very long coherence times, there is a demand for understanding the conditions for a successful growth of thin solid neon films as a qubit substrate. Therefore, in this review also the triple point wetting phenomenon of the hydrogen isotopes and neon is discussed, which dominates the growth of solid films of these materials.

**Keywords** Surface electrons · Quantum solids · Quench-condensed films · Triple point wetting · Electron-on-neon qubit

## 1 Introduction

Electrons in surface states above inert quantum surfaces have been studied as an example of a particularly clean and well-defined model system for condensed matter physics since more than half a century. Based on the theoretical work by Cole and Cohen [1, 2] and at about the same time by Shikin [3, 4] about the formation of hydrogen-like bound states in the vacuum above the quantum liquids and solids helium, hydrogen, and neon, a vast body of experimental and theoretical studies has been accomplished [5]. The emphasis was particularly on superfluid <sup>4</sup>He as a substrate, and the investigated phenomena include the transition to excited states, the phase transition from a 2-dimensional electron liquid to a solid (the Wigner crystal), and the many aspects of the (magneto-) transport properties of 2D electron systems [6–8]. Altogether, as a result of these studies, electron ensembles on liquid helium can be considered as quite well understood.

---

✉ Paul Leiderer  
paul.leiderer@uni-konstanz.de

<sup>1</sup> Fachbereich Physik, Universität Konstanz, 78457 Constance, Germany

In 1999, Platzman and Dykman [9] suggested to use surface state electrons on liquid  $^4\text{He}$  as qubits for quantum computing. Considering the purity of this system, this appeared as a promising route for qubits with long coherence times. After significant efforts and also remarkable progress, however, it was realized that fluctuations of the liquid level as well as the coupling between the electrons and excitations of the superfluid surface (ripples) can lead to rapid decoherence [10–12]. It should be possible to avoid this problem by using solid neon as a substrate for the electron qubit instead of superfluid helium. Indeed, recent experiments with electrons on solid neon have demonstrated coherence time orders of magnitude longer than achieved so far for charge qubits in semiconductors and superconductors [13–16]. This brief review is motivated by these experiments and focuses in the first part on early investigations of electron ensembles above the quantum solids hydrogen and neon, and in the second part on the phenomenon of triple point wetting, which is relevant if one wants to grow solid films of neon as a qubit substrate.

## 2 Early Experiments with Electrons on the Surface of Hydrogen and Neon

### 2.1 Electrons on the Bulk Crystal Surface

The first experiments with electrons above the quantum solids hydrogen and neon have been reported by the group of Khaikin [17, 18]. They determined the electron mobility on these substrates by using the Sommer-Tanner geometry established already for electrons on liquid helium [19]. The principle of this technique, sketched in Fig. 1 (left) and in the insets in Figs. 2 and 3, is to periodically move the electrons along the liquid or crystal surface by means of segmented capacitor plates (with an area in the  $\text{cm}^2$  range). Results for the hydrogen crystals are shown in Fig. 1 (right). At temperatures well below the triple point temperature of  $\text{H}_2$ , 13.9 K, the mobility was found to be nearly constant, somewhat above  $10^4 \text{ cm}^2/\text{Vs}$ , which according to the authors is given by scattering from surface defects. For comparison, the mobility of electrons on bulk liquid He is  $> 10^6 \text{ cm}^2/\text{Vs}$  at temperatures below 1 K [5], where scattering from liquid surface excitations (“ripples”) is the dominant mechanism. An estimate for the scattering from surface excitations at the solid hydrogen surface (Rayleigh waves), presented by the authors, yields a contribution two to three orders of magnitude smaller than scattering from surface defects and was therefore not observable in this experiment. At  $T > 10 \text{ K}$ , the mobility drops steeply due to the increasing contribution of scattering from gas molecules.

Surface electrons on solid neon at relatively high densities up to  $3 \times 10^{10} \text{ cm}^{-2}$  (about an order of magnitude higher than the critical density on bulk liquid helium [20]) were studied a few years later by Kajita and Sasaki [21, 22]. In this work, it was shown that at high electron density and at low temperature correlations between the electrons come into play, leading eventually to Wigner crystallization of the electrons, which manifests itself in an additional lowering of the mobility. Moreover, it was demonstrated that if a thin helium film is condensed onto the neon, the

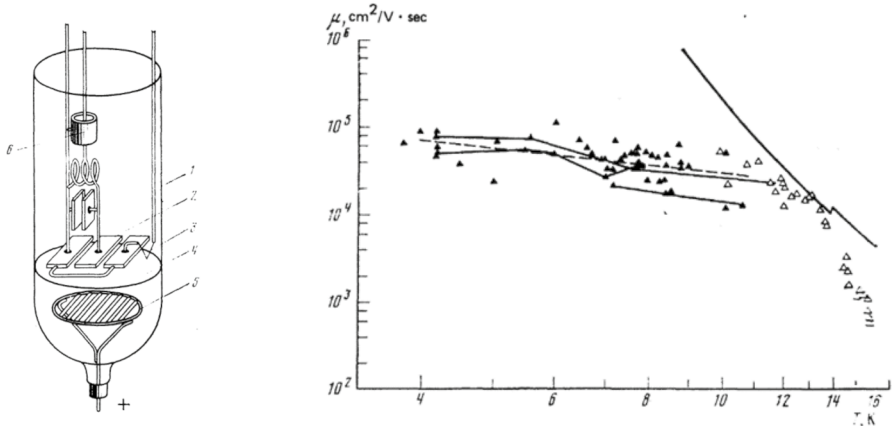


**Fig. 1** *Left:* Diagram of the apparatus used in Ref. 18. (1) Glass ampoule; (2) Upper plate; (3) Filament; (4) Hydrogen level; (5) Lower plate; *right:* mobility of electrons over the surface of solid hydrogen. Open triangles—data of Ref. 17; full triangles—data obtained in Ref. 16; right-hand solid curve—calculation of mobility due to scattering by gas molecules, dashed—average value of the mobility. The melting temperature of hydrogen is 13.9 K. The kink in the calculated curve corresponds to the jump of the dielectric constant at the melting point. (Reproduced with permission from [18])

electrons above the He film break through to the solid substrate, if their density is high, but they can be lifted again if the film is pumped off and then condensed anew.

Another experiment with electrons on a  $^4\text{He}$  supported by a weakly-binding substrate—in this case again solid hydrogen—was carried out by Paalanen and Iye [23]. Naively, one might have expected that the helium film smoothens the existing roughness of the crystal surface, so that the mobility would increase upon the addition of helium. However, the experiment showed that the mobility on the film is *smaller* than on bare  $\text{H}_2$  or also on the bulk liquid helium surface. The additional scattering is due to the density fluctuations in the uppermost He monolayer. Whenever a layer is completed, these density fluctuations are minimal, leading to a maximum in the mobility. The oscillations in the mobility shown in Fig. 2 therefore reflect the layer-wise growth of the He film on the  $\text{H}_2$  crystal surface.

In a similar experiment by Cieslikowski et al. [24] up to 9 of these oscillations were observed—which was kind of surprising, because it had not been expected that layering in a liquid extends over such large distances. In the same experiment, starting at high temperatures from the liquid  $\text{H}_2$  phase (Fig. 3), the solidification at the triple point temperature was clearly seen as a sharp drop in the electron mobility  $\mu$ , showing that the crystal was not as smooth as the liquid surface, an indication of the surface defects already mentioned by Troyanovskii et al. [18]. The height of this jump was somewhat different from one crystal to the other, as expected. The increase in  $\mu$  upon lowering the temperature reflects the decrease in the  $\text{H}_2$  gas atom density. The dip around 8 K was qualitatively reproducible from crystal to crystal; its origin remains unknown, however. The typical mobility on the bare crystal at low T was again in the range of  $10^4$   $\text{cm}^2/\text{Vs}$ , like in the previous experiments.

**Fig. 2** Normalized electron mobility for unsaturated He films as a function of He pressure. The results at different temperatures, from bottom to top, are from the 19th, 25th, and 26th H<sub>2</sub> crystals with  $\mu_0 = 4.0, 2.3,$  and  $1.7 \text{ m}^2/\text{Vs}$ , respectively (reproduced with permission from [23])

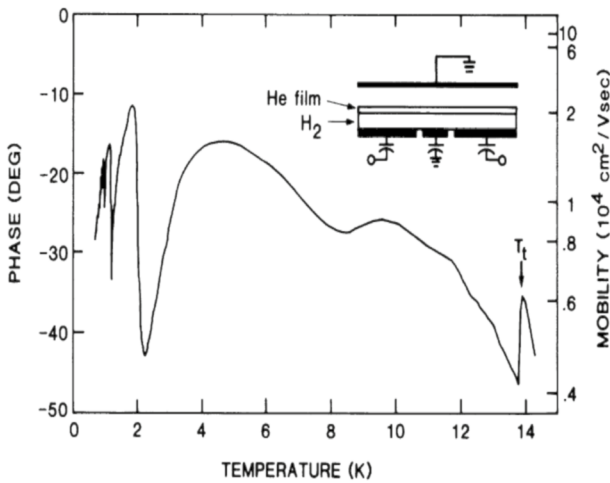
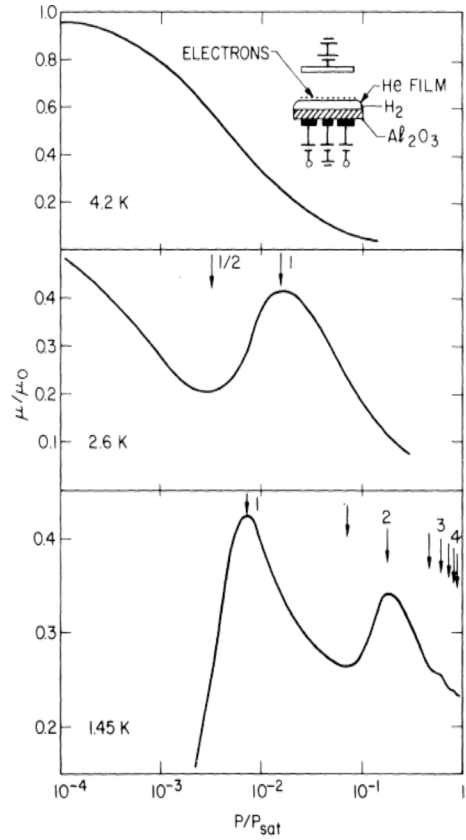


**Fig. 3** Phase shift for electrons on solid H<sub>2</sub> covered by a He film with a temperature-dependent thickness. The He gas pressure was 0.35 mbar at 5 K. The electron mobility is given on the right-hand scale. Inset Sketch of the sample cell (reproduced with permission from [24])

## 2.2 Electrons on Quench-Condensed Films

As the results discussed so far demonstrate, growing hydrogen and neon crystals near thermodynamic equilibrium from the bulk liquid by slowly lowering the temperature through the triple point gives surfaces with reasonable quality for electron mobility measurements. The thickness of the solid  $H_2$  or Ne in those experiments was on the order of 1 mm. Much thinner films in the some ten to hundred nm range, as one would need them for qubit purposes, cannot be prepared in this way from the liquid phase. The challenge therefore is to grow thin smooth quantum solid films from the gas phase. In thermodynamic equilibrium, however, it is not possible to grow solid hydrogen or neon films thicker than just a few molecular or atomic monolayers, respectively, because both species are subject to the phenomenon of triple point wetting, as described in the next chapter. In experiments by Kono et al. [25, 26], a different route was therefore tried, namely preparing the quantum film by quench condensation of the gas atoms/molecules on a proper substrate (e.g., glass) at a temperature well below the triple point (typically around 1.5 K), and then thermally anneal the film in order to improve the surface quality. A sketch of the sample cell is shown in Fig. 4.

The virgin quench-condensed films with a thickness of about 2  $\mu\text{m}$  before any heat treatment were optically smooth, but nanoscopically rough and probably porous [27–29], so that surface electron currents could not be detected. Only upon raising the temperature to about 3.5 K resulted in a measurable conductivity, which could be enhanced further by additional annealing steps (Figs. 5, 6).

The arrows in Fig. 5 indicate the first warming up to 8 K and the subsequent cooling. Obviously, the surface quality was improved by the annealing process, so that a measurable electron conductivity was found down to about 2 K. Repeated annealing steps (Fig. 6) led to further improvement, but the mobility was still well below the values for bulk  $H_2$  crystals. The temperature dependence above 2 K could be described by a thermally activated process with activation energies between 23 and 10 K. The steep increase in the conductivity below 2 K came from the condensation

**Fig. 4** Schematic drawing of the experimental cell.  $E_1$  and  $E_2$  are concentric electrodes.  $G$  is the glass substrate and  $I$  is an insulating sheet.  $H_1$  and  $H_2$  are manganin heaters and  $T_1$ ,  $T_2$ , and  $T_3$  are carbon resistors. Hydrogen enters the cell from the top through a capillary (reproduced with permission from [25])

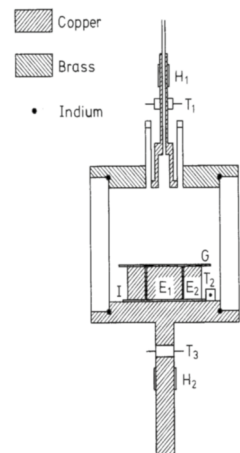


**Fig. 5** Behavior of the surface electron conductivity  $\sigma$  during the first annealing process after the quench-condensation of the hydrogen substrate. Arrows indicate the direction of the chronological development (reproduced with permission from [30])

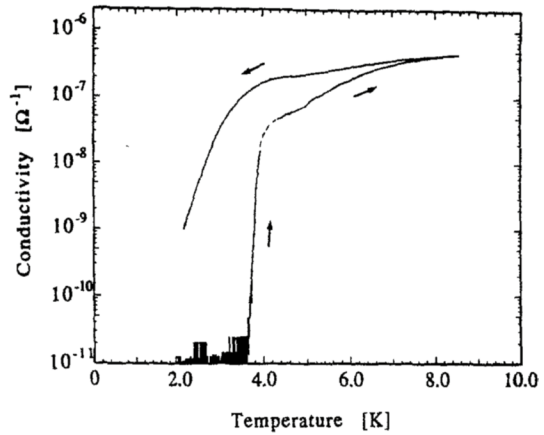
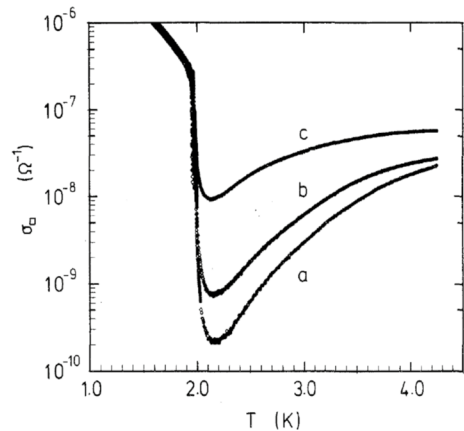


**Fig. 6** Conductivity of surface electrons on hydrogen substrates annealed in three stages **a** after annealing the film at 4.2 K for 1 h; **b** after annealing at 4.2 K for 12 h; **c** after annealing at 8 K for 1 h (Reproduced with permission from [26])



of He gas atoms to a liquid film, which was studied in analogy to the layering oscillations on bulk hydrogen [23, 24]. In the case of the quench-condensed  $H_2$  films of Ref. [26]; however, layering was not observed because the hydrogen was apparently still too rough even after annealing.

An interesting feature during the growth of the helium film upon cooling—hardly discernible in the steep increase in Fig. 6—becomes apparent in the blow-up in Fig. 7: A local maximum followed by a sharp dip in the conductivity. This feature has been interpreted by Monarkha and coworkers [31] in terms of a rough substrate surface, as a transition from a state where the electrons are localized in the valleys of the substrate (when the film is thin) to the tops of the bumps (when the film is thick) (Fig. 8). Trapping of an electron at a bump also has been suggested very recently for the observed electron-on-neon qubit [32].

In follow-up experiments somewhat later the surface quality of the quench-condensed  $H_2$  films could be sufficiently improved that the electron mobility in the dilute case reached  $0.5 \times 10^4 \text{ cm}^2/\text{Vs}$  [33]. On these solid film substrates, clear evidence for

**Fig. 7** Expanded view of Fig. 6. Note that the temperature of the dip is not affected by the annealing process (reproduced with permission from [26])

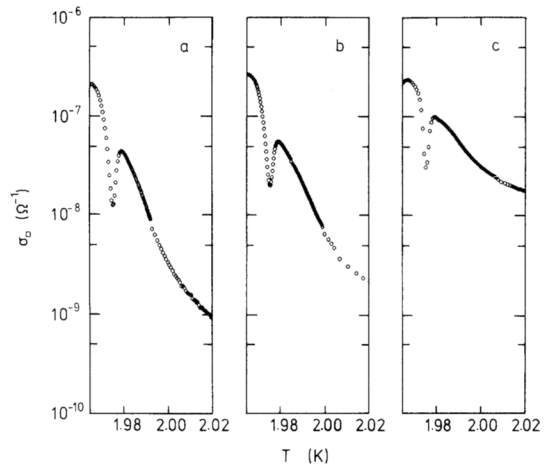
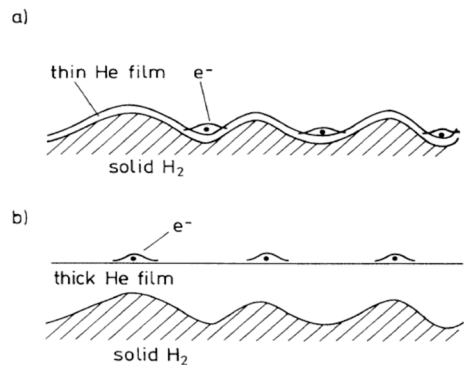


**Fig. 8** Schematic sketch of the two states involved in the structural transition of the surface electrons above a rough solid substrate covered with a helium film. **a** Surface electrons are localized in the valleys of the surface roughness. **b** Surface electrons are localized opposite the tops of the solid surface roughness (Reproduced with permission from [31])



Wigner crystallization at high electron densities around a plasma parameter  $\Gamma \sim 125$  was found, similar to the results for the *bulk* Ne crystal surface by Kajita [22]. It should be mentioned that analogous experiments with surface electrons on quenched/annealed Ne films have—to our knowledge—not been carried out yet.

### 3 Triple Point Wetting of Hydrogen and Neon

#### 3.1 Films in Thermodynamic Equilibrium

As already mentioned,  $H_2$  and Ne exhibit the so-called triple point wetting. This phenomenon, which applies also to other noble and molecular gases, can be characterized by the adsorption isotherms of these elements (i.e., the variation of the film thickness of the adsorbate on a solid substrate as the gas pressure of the adsorbate is increased up to saturated vapor pressure (svp)  $p_0$  at constant temperature): above the triple point temperature, the film thickness  $d$  diverges for

**Fig. 9** Adsorption isotherms of Kr on Au(111) below its triple point. For clarity, successive curves have been shifted upward by 13 Hz. The film thickness is proportional to the plotted frequency change  $\Delta f$  of the microbalance circuit.  $P/P_0$  is the reduced pressure. (comment by the author  $T_t$  is here the triple point temperature, and the area of the microbalance crystal (and hence the area of the probed film) was macroscopic, in the  $\text{cm}^2$  range)(reproduced with permission from [34])

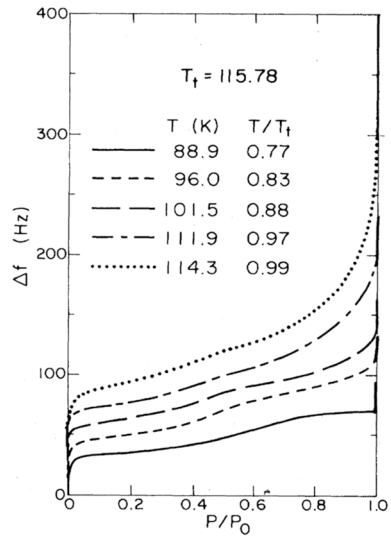
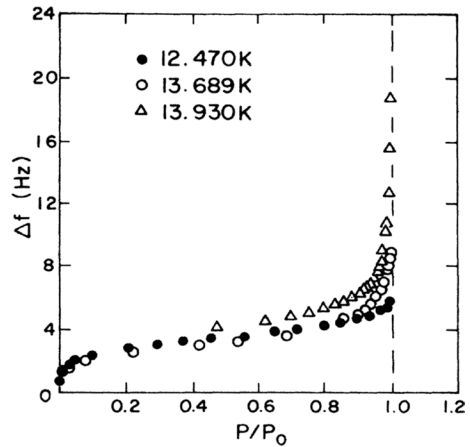


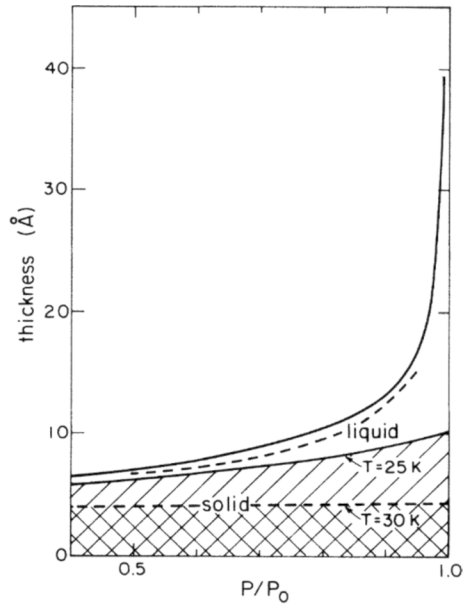
**Fig. 10** Adsorption isotherms of  $\text{H}_2$  on Au (111) near its triple point. Plotted is the frequency change  $\Delta f$  versus  $P/P_0$  for three temperatures below  $T_3$  (reproduced with permission from [36])



$p \rightarrow p_0$  (“complete wetting”), while  $d$  remains finite at svp for temperatures below  $T_3$  (“incomplete wetting”). Triple point wetting has been studied, among others, in a series of pioneering experiments by the groups of Dash and Vilches [34–36] using a high-frequency microbalance technique. Examples for Kr and  $\text{H}_2$  are shown in Figs. 9 and 10.

The transition from incomplete to complete wetting was found to be continuous, the maximum thickness  $d$  of the layered films below  $T_3$  varying as  $d \sim (1 - T/T_3)^{-1/3}$ . The interpretation for this behavior, given in Ref. 35, is at first sight surprising: It is suggested that the rise in film thickness (approaching  $T_3$  from below) close to  $T_3$  is not due to an increase of the *solid* film thickness, but to a *liquid* phase which makes up most of the thick film (sketched in Fig. 11). (The reason

**Fig. 11** Liquid and solid layer thicknesses of neon films on Ag as function of reduced pressure, calculated according to the slab model. The double-hatched region marks the solid layer thickness at  $T=30$  K, and the single-hatched region marks the solid thickness at 25 K. The solid and dashed lines correspond to the total thicknesses at 25 and 30 K, respectively (reproduced with permission from [35])

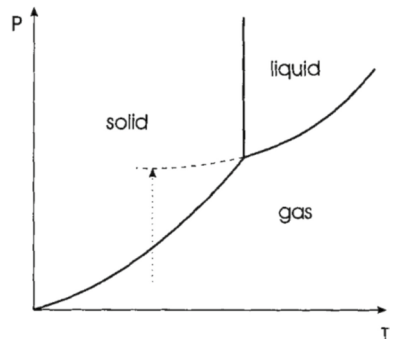


why the solid part of the adsorbed film is restricted to a few monolayers due to strain in the crystalline layer will be discussed further below.)

In order to visualize the observed power law dependence of  $d$  below  $T_3$ , we consider the schematic phase diagram as depicted in Fig. 12 [37]. The liquid–gas coexistence line represents the intersection of the free energy surfaces of the liquid and the gaseous phase. The chemical potential  $\mu$  of the atoms/molecules in the sample cell, measured with respect to the coexistence value  $\mu_{\text{coex}}$ , is given by

$$\Delta\mu = \mu - \mu_{\text{coex}} = k_B T \ln \left( p/p_0^{\text{liq}} \right) \tag{1}$$

**Fig. 12** Schematic phase diagram of hydrogen and the noble gases. The liquid/gas coexistence curve is extrapolated into the solid phase region (dashed line). The dotted line indicates the path of an adsorption isotherm, extrapolated up to liquid/gas coexistence (reproduced with permission from [37])



where  $k_B$  is Boltzmann's constant. Condensation of the liquid phase will occur when the saturated vapor pressure  $p_0^{\text{liq}}$  is reached, i.e., when  $\Delta\mu=0$ . Close to the substrate, the atoms/molecules are in addition subject to the van der Waals potential, which varies as  $d^{-3}$ ; hence, this interaction with the substrate contributes to the chemical potential of the adsorbate as

$$\Delta\mu_{\text{vdW}} = \alpha/d^3 \quad (2)$$

where  $\alpha$  denotes the van der Waals constant. The combination of Eqs. (1) and (2) leads to

$$d = \left[ \alpha/k_B T \ln \left( p/p_0^{\text{liq}} \right) \right]^{1/3} \quad (3)$$

For the gas pressure  $p$  being close to  $p_0^{\text{liq}}$ , the liquid film thickness therefore varies as

$$d \sim \left( p_0^{\text{liq}} - p \right)^{-1/3} \quad (4)$$

In Fig. 12, the liquid–gas coexistence line is extended by the dashed line into the solid phase region. In addition, the dotted line traces the pressure of a (hypothetical) adsorption isotherm, extrapolated beyond the solid–gas coexistence up to the extrapolated liquid–gas coexistence. We know from the data above  $T_3$  that the film thickness diverges according to Eq. (4) when the liquid–gas coexistence line is approached. Below  $T_3$ , however, this line cannot be reached in thermodynamic equilibrium: if, in a gedankenexperiment, we slowly increase the gas pressure in the sample cell along the dotted line, the maximum pressure that is accessible is  $p_0^{\text{sol}}$ , the saturated vapor pressure of the solid phase. If more gas will be added to the sample cell, a bulk crystal will start to form somewhere in the cell at constant pressure  $p_0^{\text{sol}}$ , and the thickness of the liquid film will not increase further. Since below the triple point, the pressure difference  $p_0^{\text{liq}} - p_0^{\text{sol}}$  varies approximately as  $T_3 - T$  close to  $T_3$  (see Fig. 12), Eq. (4) then yields  $d \sim (1 - T/T_3)^{-1/3}$ , as observed in Refs. 34–36. For  $T < T_3$ , no liquid film remains, and as a result just a solid film only a few monolayers thick is formed even at svp.

These microbalance studies of triple point wetting have been complemented a few years later with investigations using the optical techniques surface plasmon resonance (SPR) spectroscopy and ellipsometry [30, 38, 39]. The area of the adsorbed films was again macroscopic, the spot probed by the optical beam being about  $1 \text{ mm}^2$ . Also in these measurements it was found that the equilibrium thickness  $d$  of hydrogen and neon films dropped below the triple point temperature, following a power law  $d \sim (1 - T/T_3)^{-1/3}$ , as shown in Fig. 13 [30].

Such a behavior even pertains to isotopic mixtures, as studied for the case of the  $\text{H}_2$ – $\text{D}_2$  system [38]. The triple point temperature of these two isotopes is quite different, for pure  $\text{H}_2$  it is 13.9 K, and for pure  $\text{D}_2$  the value is 19 K. For mixtures, it turns out that one has an effective triple point which depends on the isotopes' concentration, and the drop according to  $d \sim (1 - T/T_3)^{-1/3}$  occurs at that “effective” triple point temperature (Fig. 14). Thus, it is not possible to change the qualitative

**Fig. 13** Film thickness  $d$  versus the reduced temperature (with respect to the triple point temperature  $T_3$ ). The dashed lines represent a behavior  $d \sim (1 - T/T_3)^{-1/3}$  (reproduced with permission from [30])

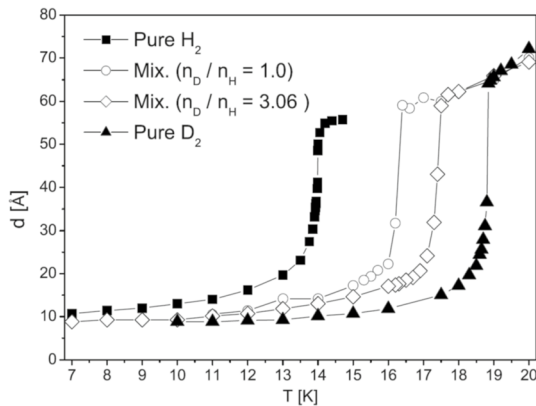
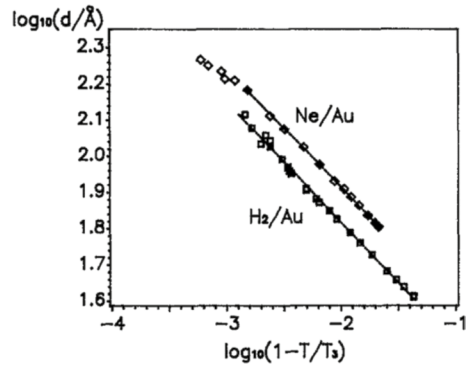


**Fig. 14** Wetting curves of pure and mixed systems of  $H_2$  and  $D_2$ . The data demonstrate the existence of an effective triple point,  $T_3^{(eff)}$ , which depends on the species concentration of the  $H_2$ – $D_2$  mixture. The value of  $T_3^{(eff)}$  always falls between  $T_3^{(H_2)}$  and  $T_3^{(D_2)}$ . The fact that the maximum film thickness above  $T_3$  does not really diverge but saturates at a large but finite thickness is ascribed to minute temperature gradients in the sample cell and the height difference between the film surface and the bulk material, which give rise to a sample pressure slightly below svp [35] (reproduced with permission from [38])

behavior of this quantum system and produce *thick* solid hydrogen isotope films in thermodynamic equilibrium by mixing different species. Rather, in all investigated cases the film thickness at  $T < T_3$  was only about 1 nm, i.e., 2–3 molecular layers.

One reason for the finite thickness of a solid film (incomplete wetting) of an adsorbate–substrate system which exhibits complete wetting in the liquid state is that a solid cannot relax the elastic compression caused by the substrate attraction. This leads to an additional contribution in the free energy, a measure being the (reduced) Hamaker constant  $R$  (the ratio between adsorbate–substrate and adsorbate–adsorbate interaction). On this basis, Gittes and Schick have developed a theory [40] which describes the solid adsorption on a flat substrate. It predicts that for a particular value  $R = R_0$  complete wetting is possible, while for  $R > R_0$ , in contrast to liquid wetting, the thickness of the solid film decreases with increasing  $R$ . A result of this

theory for the  $H_2$  adsorbate is shown in Fig. 15 as a function of  $R$  (solid curve). For the substrates used in the experiments of Figs. 13 and 14 (Au) the calculated value of  $R$  is 4.5, one therefore would expect a solid  $H_2$  thickness of 10 nm at svp (but not the experimentally observed value of about 1 nm). Moreover, the maximum thickness should increase when  $R$  is reduced, which can be achieved by preplating the gold substrate with thin films of weakly interacting substances like the rare gases.

Results of such a preplating experiment with Ne, Ar, and also the molecule  $CH_4$  as preplating agents are plotted in Figs. 16 and 17. As the data show, an influence of preplating is visible indeed: For  $CH_4$  a 50% increase in the  $H_2$  layer is observed at  $T < T_3$ , while for Ne, preplating films decreases the equilibrium film thickness. For Ar preplating, the  $H_2$  thickness is the same as on bare gold within the

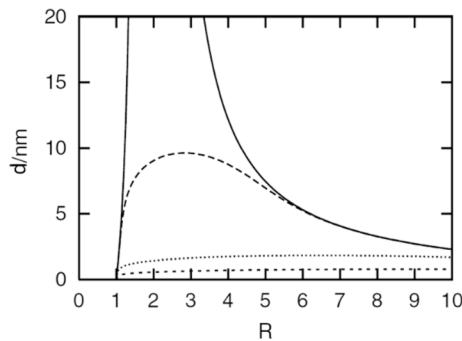


**Fig. 15** Theoretical thickness  $d$  of the adsorbed hydrogen layer at solid–gas coexistence for  $T/T_3=0.6$  as a function of the reduced substrate strength  $R$ . Solid line Gittes–Schick theory. The dotted and dashed lines are for different nonvanishing surface roughnesses,  $G=10^{-2}/\sigma^2$ ,  $G=10^{-4}/\sigma^2$ , and  $G=10^{-8}/\sigma^2$  (bottom to top) as calculated by Esztermann et al. [41]. (reproduced with permission from [41])

**Fig. 16** Wetting curves of pure  $H_2$  on Au and when preplated with Ne and Ar (reproduced with permission from [39])

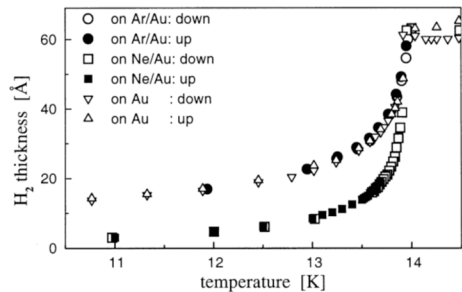
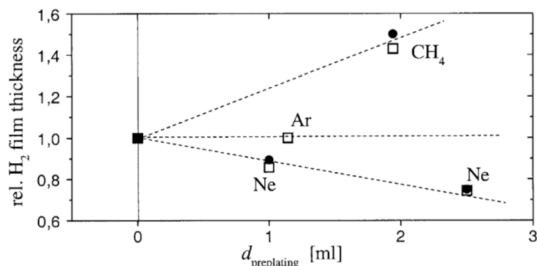


**Fig. 17** Maximum  $H_2$  film thickness (at saturated vapor pressure) for various preplating layers – with  $H_2$  on bare Au as reference. Dashed lines are just a guide to the eye (reproduced with permission from [39])



experimental resolution. The overall behavior, namely a thick, wetting  $H_2$  film above the triple point temperature and gradual dewetting below  $T_3$  is also observed for preplated substrates. The main result is that for all combinations of preplated material the equilibrium film thickness—apart from small effects—is the same as without preplating.

This indicates that the picture of wetting of solid films as described by the Gittes–Schick theory is incomplete. Esztermann et al. [41] therefore consider in addition the influence of possible roughness of the solid substrate. In fact, the evaporated gold and silver films which have been used in the described wetting studies [34–39] are usually quite rough, typically consisting of “hills” some hundred nm wide and some ten nm high. An example is shown in Fig. 18a. The strain induced in the adsorbed film by the bending due to this roughness gives rise to an additional term in the free energy of the system. Results calculated in Ref. 41 are shown in Fig. 15 for different roughness parameters  $G \sim h^2/b^4$ , where  $b$  is the characteristic lateral length scale of the surface modulation and  $h$  is the vertical (valley to peak) height. The roughness  $G$  calculated from the profile plotted in Fig. 18a is  $G = 5.4 \times 10^{-4}/\sigma^2$ , with  $\sigma$  denoting a molecular length scale. It is seen that for  $G$  in this range the expected solid thickness at svp calculated by Esztermann et al. is much smaller than the 10 nm calculated on the basis of the Gittes–Schick theory, in qualitative agreement with experiment. Furthermore, the fact that a variation of  $R$  does not have a big influence on the solid layer thickness for roughness parameter values  $G \geq 10^{-4}/\sigma^2$  is in accord with the preplating measurements in Fig. 17.

As a further test of the influence of a rough surface, a gold substrate with reduced roughness has been studied (Fig. 18b). As predicted by the theory of Ref. 41, a slight increase in the equilibrium  $H_2$  thickness has been found. An even smoother surface, as provided by a commercial silicon wafer, was studied in Ref. 38 (see Fig. 19).

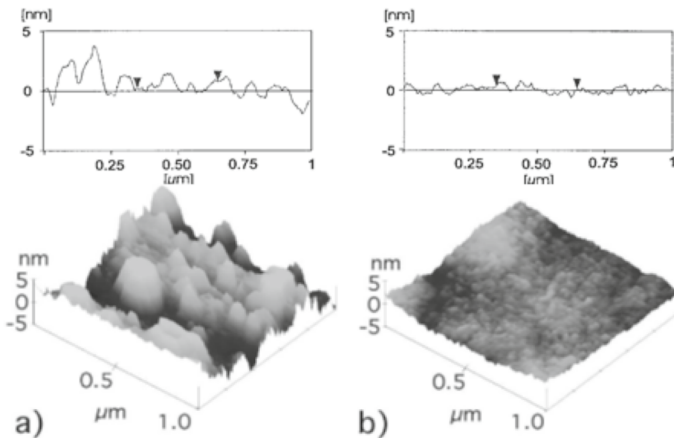


**Fig. 18** **a** A typical 1000 nm × 1000 nm atomic force microscope image of a Au film evaporated at room temperature on glass; the top shows a line scan of this image; **b** with the same resolution generated AFM-image of a Au surface, which this time, however, had been detached from a Si wafer (reproduced with permission from [41])

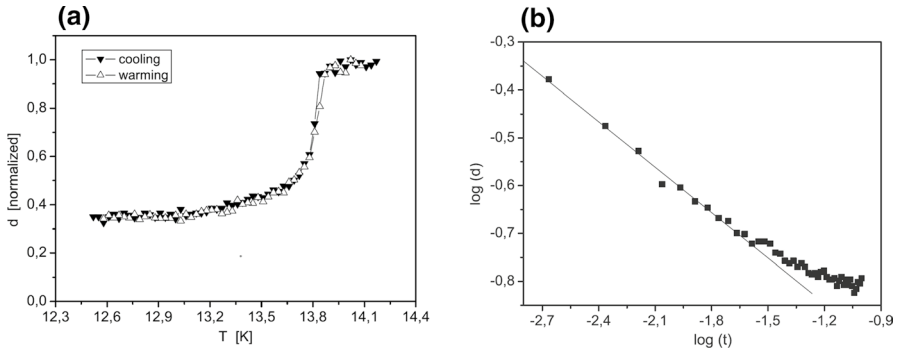


**Fig. 19** **a** Triple point wetting of  $\text{H}_2$  on a smooth Si wafer. The thickness  $d$  is normalized to the thickness in saturation above  $T_3$  of  $\text{H}_2$ . The full symbols are for cooling, and the open symbols are for warming. **b** Warming curve of Fig. 19 **a** plotted on a logarithmic scale. The slope of the straight line is 0.31 (reproduced with permission from [38])

It was found that at  $T \ll T_3$  an increase from about 3 to 7 solid layers (1 nm to 2.5 nm) is observed compared to Au films. A further increase in the solid  $\text{H}_2$  thickness by about 2 monolayers was measured on laser-annealed Si surfaces [38].

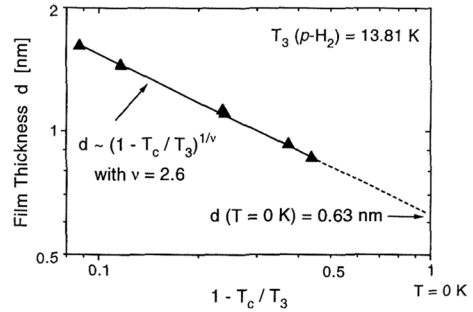
The adsorption measurements discussed so far were all carried out on macroscopically plane (although nanoscopically rough) substrate surfaces. One might argue that on devices for qubits [13, 14] one is dealing with structured surfaces, where due to the local curvature of the substrate the surface tension of the adsorbate adds to the energy budget and gives rise to a “capillary effect.” Although this is true, for channels with a typical width in the micron range and targeted neon film thicknesses around 10 nm [13] the surface tension of neon should not play a decisive role. An extreme example is an experiment in Vycor glass (a porous glass with a typical pore radius 4 nm) carried out by Schindler et al. [42]: It was found in a torsion oscillator experiment that a Vycor sample completely filled with liquid  $\text{H}_2$  above the triple point, in thermodynamic equilibrium lost a major part of the hydrogen when cooled below the triple point. The  $\text{H}_2$  film thickness, extrapolated to 0 K, was 0.63 nm, in qualitative agreement with the results for a plane, but nanoscopically rough surface (Fig. 20). This is also expected, because the argument by Esztermann et al. that the local strain generated by surface roughness adds to the free energy of the system applies for the nano-channels in the Vycor glass as well [42].

Recent experiments in Konstanz with the noble gas Ar in channels 1.7  $\mu\text{m}$  wide and 1.2  $\mu\text{m}$  deep are also in agreement with the triple point wetting results for plane substrate surfaces [43]

### 3.2 Annealing of Quench-Condensed Films

Quench-condensed quantum matter films have already been mentioned in the context of surface electron studies. In addition, such films have also been investigated in separate experiments with the surface plasmon resonance technique. Such measurements not only provide information about the film thickness (via the shift of the

**Fig. 20** Film thickness of hydrogen adsorbed on Vycor as a function of the corresponding reduced characteristic temperature  $T_c/T_3$  ( $T_c$  being a thickness-dependent characteristic temperature below which the  $H_2$  molecules start to escape from the Vycor pores (reproduced with permission from [42])



SP resonance angle), but they allow also some conclusions about the roughness of the adsorbed film (on the scale of the wavelength of the SPR laser). The films were in this case thinner than in the experiments mentioned in chapter 2.2 (on the order of 100 nm instead of several  $\mu\text{m}$ ), because the SPR technique is only sensitive on length scales of the laser wavelength or smaller. Surface electron studies were not possible with such thin quench-condensed films since for that small thicknesses electrons penetrate the films because of their open structure.

An example for the annealing of quench-condensed  $H_2$  and  $D_2$  films measured by SPR is shown in Fig. 21 for films with an initial thickness of 125 nm [44]. In Fig. 21a, the shift of the resonance angle (plotted as an optical thickness, assuming that the film has the bulk hydrogen density) is plotted versus the increase in temperature. The rate of temperature increase was always slow enough that the films were close to thermal equilibrium. The preparation temperature of the films was 1.5 K. Below about 2.8 K for  $H_2$  and 4.4 K for  $D_2$ , the signal for the film thickness is constant, indicating that the films remain in a metastable state. Above these temperatures, however, the molecules become mobile, rearrange and form crystallites with a size distinctly larger than the original film thickness, which leads to a drop in the apparent SPR-measured film thickness (Fig. 21a). In the same temperature range, the width of the SP resonance broadens, due to scattering of the surface plasmons at the crystallites (Fig. 21b). An additional measurement of the scattered light also exhibits a strong increase in the same temperature interval, and, moreover, an anisotropy between forward and backward scattering direction, which indicates that the size of the crystallites is comparable to or larger than the laser wavelength (Fig. 21c). Finally at a temperature of 3.8 K for  $H_2$  (and 5 K for  $D_2$ ) the molecules start to thermally desorb.

In an analogous SPR-experiment with neon such as coarse graining effect was not observed, both the thickness signal and the SPR width remained constant up to desorption which set in around 7.5 K (Fig. 22) [30]. This difference is surprising, considering the otherwise quite similar triple point wetting properties of hydrogen and neon.

Results for the annealing of quench-condensed  $H_2$  films have also been obtained by Classen et al. [45] using surface acoustic (Rayleigh) waves. Also their data indicate that at temperatures far below the triple point such films undergo drastic structural changes, forming larger crystallites of typically 1  $\mu\text{m}$  diameter.

**Fig. 21** Quench-condensed H<sub>2</sub> and D<sub>2</sub> films on Au versus temperature during warming: **a** surface plasmon resonance (SPR) position (optical thickness; **b** broadening of the plasmon resonance; **c** scattered light intensity at two scattering vectors (forward: 3.7 μm<sup>-1</sup>, backward: 19.5 μm<sup>-1</sup>) (reproduced with permission from [44])

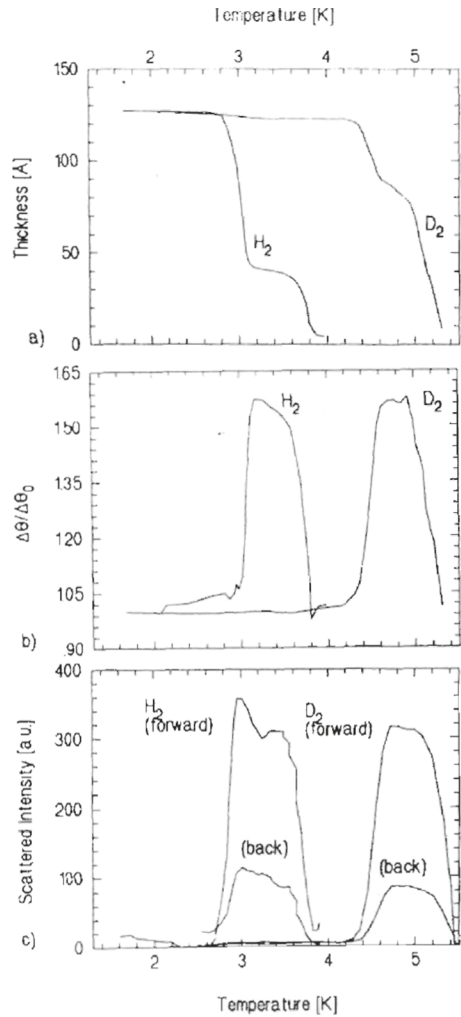
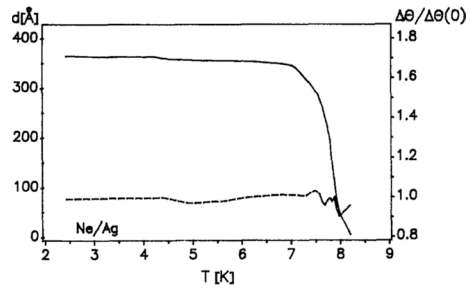


**Fig. 22** Apparent optical thickness (*full line*) and reduced surface plasmon width (*dashed line*) of a quench-condensed Ne film versus temperature during warming (reproduced with permission from [30])



The rearrangement of the film structure could be traced in situ by changes of sound velocity and attenuation arising from scattering of the Rayleigh waves by inhomogeneities. The authors conclude that the dominant scattering mechanism appears to be well described by a resonant interaction between surface acoustic waves and elastic eigenmodes of the hydrogen crystallites ("surface shape resonances").

## 4 Conclusions and Outlook

The experiments carried out so far with ensembles of surface electrons on hydrogen and neon have shown that these quantum solids are in principle suitable substrates for electrons. Phenomena like layering of liquid helium next to a solid wall and correlation effects between the electrons at high densities including Wigner crystallization could be demonstrated. Since the surface quality of these quantum crystals is not perfect, however, defects limit the electron mobility due to scattering and trapping, and hence also the reproducibility of the transport measurements. This is one of the reasons why studies of surface electrons on hydrogen or neon are much less numerous than on liquid helium.

As discussed in chapter 3 of this review, a straightforward growth of smooth solid neon films more than a few monolayers thick is not possible in thermodynamic equilibrium because these films undergo triple point wetting, originating from strain caused by the substrate of the film, in particular due to surface roughness. One should be able to increase the equilibrium film thickness somewhat by preparing the device surfaces as smooth as possible. Quench-condensed films, on the other hand, can be grown to arbitrary thickness, but they are typically very rough and must be annealed to improve the surface quality. This annealing can lead to crystallites (or "bumps") on the film surface, and the smoothness of such surfaces will depend on the details of the annealing process. Studies for optimizing the film preparation are presently underway [46]. In spite of these problems, electron-on-neon qubits with attractive properties have already been demonstrated [13, 14]. Actually, the trapping of electrons at bumps on the crystal surface is not necessarily detrimental for such qubits, as has been shown in the recent publication [32].

**Acknowledgements** Close collaborations with Arnie Dahm, Kimitoshi Kono, Hartmut Löwen and Valeri Shikin are gratefully acknowledged. The author has profited a lot over the years working with the group members U. Albrecht, D. Cieslikowski, R. Conrath, W. Ebner, S. Herminghaus, J. Klier, F. Mugele, M. Souhaili, and C. Weichhard.

**Author contributions** PL has selected the material for this review and has written the manuscript

**Funding** Open Access funding enabled and organized by Projekt DEAL.

**Data availability** No datasets were generated or analysed during the current study.

## Declarations

**Competing interests** The authors declare no competing interests.

**Open Access** This article is licensed under a Creative Commons Attribution 4.0 International License, which permits use, sharing, adaptation, distribution and reproduction in any medium or format, as long as you give appropriate credit to the original author(s) and the source, provide a link to the Creative Commons licence, and indicate if changes were made. The images or other third party material in this article are included in the article's Creative Commons licence, unless indicated otherwise in a credit line to the material. If material is not included in the article's Creative Commons licence and your intended use is not permitted by statutory regulation or exceeds the permitted use, you will need to obtain permission directly from the copyright holder. To view a copy of this licence, visit <http://creativecommons.org/licenses/by/4.0/>.

## References

1. M.W. Cole, M.H. Cohen, Image-potential-induced surface bands in insulators. *Phys. Rev. Lett.* **24**, 1238 (1969)
2. M.W. Cole, Properties of image-potential-induced surface states of insulators. *Phys. Rev.* **BB 2**, 4239 (1970)
3. V.B. Shikin, Motion of helium ions near a vapor-liquid surface. *Soviet Phys. JETP* **31**, 936 (1970)
4. V.B. Shikin, Some properties of surface electrons in liquid helium. *Soviet Phys. JETP* **33**, 387 (1971)
5. E. Andrei ed. *2D electron Systems on Helium and Other Cryogenic Substrates*, (Kluwer Academic, New York 1997)
6. C.C. Grimes, T.R. Brown, Direct spectroscopic observation of electrons in image-potential states outside liquid helium. *Phys. Rev. Lett.* **32**, 280 (1974)
7. C.C. Grimes, G. Adams, Evidence for a liquid-to-crystal phase transition in a classical, two-dimensional sheet of electrons. *Phys. Rev. Lett.* **42**, 795 (1979)
8. A. Blackburn, K. Djerfi, M.I. Dykman, C. Fang-Yen, P. Fozooni, A. Kristensen, M.J. Lea, P.J. Richardson, A. Santrich-Badal, R.W. van der Heijden, Magnetotransport of 2D electrons on liquid helium in the fluid and solid phases. *Czech J. Phys.* **46**(Suppl 6), 3056–3062 (1996). <https://doi.org/10.1007/BF02548110>
9. P.M. Platzman, M.I. Dykman, Quantum computing with electrons floating on liquid helium. *Science* **284**, 1967 (1999)
10. D.I. Schuster, A. Fragner, M.I. Dykman, S.A. Lyon, R.J. Schoelkopf, Proposal for manipulating and detecting spin and orbital states of trapped electrons on helium using cavity quantum electrodynamics. *Phys. Rev. Lett.* **105**, 040503 (2010)
11. Ge Yang, A. Fragner, G. Koolstra, L. Ocola, D.A. Czaplewski, R.J. Schoelkopf, and D.I. Schuster, Coupling an ensemble of electrons on superfluid helium to a superconducting circuit. *Phys. Rev. X* **6**, 011031 (2016)
12. G. Koolstra, G. Yang, D.I. Schuster, Coupling a single electron on superfluid helium to a superconducting resonator. *Nat. Commun.* **10**, 5323 (2019)
13. X. Zhou, G. Koolstra, X. Zhang, G. Yang, X. Han, B. Dizdar, X. Li, R. Divan, W. Guo, K.W. Murch, D.I. Schuster, D. Jin, Single electrons on solid neon as a solid-state qubit platform. *Nature* **605**, 46 (2022)
14. X. Zhou, X. Li, Q. Chen, G. Koolstra, G. Yang, B. Dizdar, Y. Huang, C. S. Wang, X. Han, X. Zhang, D. I. Schuster, and D. Jin, Electron charge qubit with 0.1 millisecond coherence time. *Nat. Phys.* <https://doi.org/10.1038/s41567-023-02247-5> (2023)
15. P. Stano, D. Loss, Review of performance metrics of spin qubits in gated semiconducting nanostructures. *Nat. Rev. Phys.* **4**, 672 (2022)
16. A.J. Heinrich et al., Quantum coherent nanoscience. *Nat. Nanotechnol.* **16**, 1318 (2021)
17. A.M. Troyanovskii, A.P. Volodin, M.S. Khaikin, Electron localization over the surface of crystalline hydrogen and neon. *JETP Lett.* **29**, 382 (1979)

18. A. M. Troyanovskii and M. S. Khaikin, Electron mobility in two-dimensional layer over the surface of solid hydrogen. *Sov. Phys. JETP* **54**, 214 (1981)
19. W.T. Sommer, D.J. Tanner, Mobility of Electrons on the Surface of Liquid  $^4\text{He}$ . *Phys. Rev. Lett.* **27**, 1345 (1971)
20. P. Leiderer, W. Ebner, V.B. Shikin, Macroscopic electron dimples on the surface of liquid helium. *Surf. Sci.* **113**, 405 (1982)
21. K. Kajita, W. Sasaki, Two-dimensional electrons on the helium film—solid neon system. *Surf. Sci.* **113**, 419 (1982)
22. K. Kajita, A new two-dimensional electron system on the surface of solid neon. *Surf. Sci.* **142**, 86 (1984)
23. M. A. Paalanen, Y. Iye, Electron mobility on thin He films. *Phys. Rev. Lett.* **55**, 1761 (1985)
24. D. Cieslikowski, A.J. Dahm, P. Leiderer, Investigation of thin helium films with surface-bound electrons. *Phys. Rev. Lett.* **58**, 1751 (1987)
25. K. Kono, U. Albrecht, P. Leiderer, Surface-state electrons on a hydrogen film. 1. Annealing of the film. *J. Low Temp. Phys.* **82**, 279 (1991)
26. K. Kono, U. Albrecht, P. Leiderer, Surface state electrons on a hydrogen film. 2. Influence of adsorbed helium films. *J. Low Temp. Phys.* **83**, 423 (1991)
27. K.-H. Müller, Role of the incident kinetic energy of adatoms in thin film growth. *Surf. Sci.* **184**, L375–L382 (1987)
28. M. Loistl, F. Baumann, Refractive index and mass density of quench condensed argon-xenon films. *Z. Phys. B Condensed Matter* **82**, 199 (1991)
29. N. Steinmetz, H. Menges, J. Dutzi, H.V. Löhneysen, W. Goldacker, Specific heat of disordered Xe films at low temperatures. *Phys. Rev. B* **39**, 2838 (1989)
30. P. Leiderer, U. Albrecht, Investigation of quantum systems with surface plasmons and surface state electrons. *J. Low Temp. Phys.* **89**, 2290 (1992)
31. Y.P. Monarkha, U. Albrecht, K. Kono, P. Leiderer, Helium-film-induced retrapping transition in the two-dimensional electron system above an uneven solid-hydrogen surface. *Phys. Rev. B* **47**, 13812 (1993)
32. T. Kanai, D. Jin, W. Guo, Single-electron qubits based on ring-shaped surface states on solid neon. *arXiv preprint arXiv:2311.02501* (2023)
33. F. Mugele, P. Leiderer, Wigner crystallization of two-dimensional electron systems on solid  $\text{H}_2$  films, *J. de Physique IV, Colloque C2. supplement au Journal de Physique* **13**, 45 (1993)
34. J. Krim, J.G. Dash, J. Suzanne, Triple-point wetting of light molecular gases on Au (111) surfaces. *Phys. Rev. Lett.* **52**, 640 (1984)
35. A.D. Migone, J.G. Dash, M. Schick, O.E. Vilches, Triple-point wetting of neon films. *Phys. Rev. B* **34**, 6322 (1986)
36. A.D. Migone, A. Hofmann, J.G. Dash, O.E. Vilches, Triple-point wetting of  $\text{H}_2$  films adsorbed on silver. *Phys. Rev. B* **37**, 5440 (1988)
37. S. Herminghaus et al., Hydrogen and helium films as model systems of wetting. *Ann. Phys.* **6**, 425 (1997)
38. M. Sohaili, J. Klier, P. Leiderer, Triple-point wetting of molecular hydrogen isotopes. *J. Phys. Condens. Matter* **17**, S415(2005)
39. J. Klier, C. Weichhard, P. Leiderer, Wetting behaviour of solid and liquid hydrogen films. *Physica B* **284**, 391 (2000)
40. T.F. Gittes, M. Schick, Complete and incomplete wetting by adsorbed solids. *Phys. Rev. B* **30**, 209 (1984)
41. A. Esztermann, M. Heni, H. Löwen, J. Klier, M. Sohaili, P. Leiderer, Triple-point wetting on rough substrates. *Phys. Rev. Lett.* **88**, 55702 (2002)
42. M. Schindler, Y. Kondo, F. Pobell, Mass transport of molecular hydrogen in porous vycor glass. *J. Low Temp. Phys.* **110**, 549 (1998)
43. P. Leiderer (unpublished) (2024)
44. R.N.J. Conradt, U. Albrecht, S. Herminghaus, P. Leiderer, Solid hydrogen films in a nonequilibrium state. *Physica B* **194–196**, 679 (1994)
45. J. Classen, K. Eschenröder, G. Weiss, Resonant scattering of surface acoustic waves by hydrogen crystallites. *Phys. Rev. B* **15**, 11475 (1995)
46. M.Cassiy et al., presented at the Workshop “Quantum Technologies with Floating Charged Particles” at the Okinawa Institute for Science and Technology, May 2024

**Publisher's Note** Springer Nature remains neutral with regard to jurisdictional claims in published maps and institutional affiliations.